

Numerical/Experimental Studies on Performance at Low Engine Speeds: A Case study Downsized Iranian National Engine (EF7)

Namar, Jahanian, Shafaghat & Nikzadfar, K.

Published PDF deposited in Coventry University's Repository

Original citation:

Namar, Jahanian, Shafaghat, & Nikzadfar, K 2021, 'Numerical/Experimental Studies on Performance at Low Engine Speeds: A Case study Downsized Iranian National Engine (EF7) ', International Journal of Engineering Transactions C: Aspects, vol. 34, no. 9, pp. 2137-2147.

<https://dx.doi.org/10.5829/IJE.2021.34.09C.11>

DOI 10.5829/IJE.2021.34.09C.11

ESSN 2423-7167

Publisher: Material and Energy Research Center

International Journal of Engineering (IJE) is an open access (OA) journal.

Copyright © and Moral Rights are retained by the author(s) and/ or other copyright owners. A copy can be downloaded for personal non-commercial research or study, without prior permission or charge. This item cannot be reproduced or quoted extensively from without first obtaining permission in writing from the copyright holder(s). The content must not be changed in any way or sold commercially in any format or medium without the formal permission of the copyright holders.



Numerical/Experimental Studies on Performance at Low Engine Speeds: A Case study Downsized Iranian National Engine (EF7)

M. M. Namar^a, O. Jahanian^{*a}, R. Shafaghat^a, K. Nikzadfar^{a,b}

^a Faculty of Mechanical Engineering, Babol Noshirvani University of Technology, Babol, Iran

^b School of Mechanical, Aerospace and Automotive Engineering, Coventry University, Coventry, UK

PAPER INFO

Paper history:

Received 14 April 2021

Received in revised form 19 July 2021

Accepted 30 July 2021

Keywords:

Engine Downsizing

Performance

3-Cylinder

Turbocharger

Continuous Variable Valve Timing

ABSTRACT

Engine downsizing is a trusted method to reduce fuel consumption and pollution emitted from internal combustion engines. In this method, engine displacement volume is reduced while maintaining the same power/torque characteristics. However, there still exist several limitations to utilize this technology. In this paper, the naturally aspirated type of Iranian national engine (EF7-NA) for a possible downsized version is investigated. A one-dimensional engine model equipped with a zero-dimensional two-zone combustion sub-model was developed and validated via experimental results for both natural aspirated and turbocharged engine types. Then experimental and numerical studies were carried out for the primary concept, deactivation of one cylinder besides using a turbocharger. To overcome the concept shortages, especially in lower ranges of engine speed, numerical studies were extended. Deployment of several turbochargers with different performance maps and different valve timing via a dual continuous variable valve timing (CVVT) system were investigated. The results showed that there is a feasible method for EF7 engine downsizing via a 3-cylinder type equipped with a modified turbocharger and valve timing. The maximum difference between base-engine and downsized version torque is about 7% in low engine speeds.

doi: 10.5829/ije.2021.34.09c.11

NOMENCLATURE

ID	One Dymensional	NA	Naturally Aspirated
BMEP	Brake Mean Effective Pressure	TC	Turbo-Charged
BSFC	Brake Specific Fuel Consumption	VVT	Variable Valve Timing
CR	Compression Ratio	English Symbols	
CVVT	Continuous Variable Valve Timing	A	Area, m ²
DI	Direct Injection	B	Bore, m
EGR	Exhaust Gas Recirculated	E	Internal Energy, kJ
EMS	Engine Management System	\dot{m}	Mass Flow Rate, kg/s
EVO	Exhuast Valve Opening	N	Engine Speed, rpm
GDI	Gasoline Direct Injection	T	Temperature, K
ICE	Internal Combustion Engines	V	Volume, m ³
IEA	International Energy Agency	Greek Symbols	
IVC	Inlet Valve Closing	θ	Crank Angle, deg
LHV	Low Heating Value	ρ	Density, kg/ m ³
LTC	Low Temperature Combustion	ϕ	Equivalence Ratio

1. INTRODUCTION

Engine Downsizing is well-known as a promising approach achieving the long-term goal of the

International Energy Agency (IEA) [1] focusing on a 50% reduction in mean global emission by 2030. Besides reducing the conventional emissions of Internal Combustion Engines (ICE), engine downsizing leads to

*Corresponding Author Institutional Email: jahanian@nit.ac.ir (O. Jahanian)

less carbon dioxide emission in the automotive industry, which is one of the main concerns for researchers who worked on global warming [2-4]. In this approach, the displacement volume of the engine is declined while the performance kept fixed. It is an effective solution to performance enhancement [5, 6], emission reduction [7], and frictional losses decrease [8]. Although extended researches from other aspects such as employing additives [9, 10] and Low Temperature Combustion (LTC) [11-13] were carried out to achieve IEA 2030 goals. In recent years, engine downsizing approach was succeeded in attaining outstanding emission reduction (32%) at European markets [14].

In general, downsized engines are designed based on reduction in the bore, connecting rod length, and/or the number of cylinders. It is obvious that to retaliate the performance, utilizing the boost technologies such as supercharger, turbocharger, Direct Injection (DI), and Variable Valve Timing (VVT) is essential. However, running these technologies may lead some challenges namely; knock, super-knock, pre-ignition, and also electrification [15-17].

The range of employed techniques for engine downsizing can be considered from redesigning the engine components to general new engine designing or even the Engine Management System (EMS). Although, in the recent years, the researches focus is shifted to coping the operational challenges and performance improvement rather than redesigning [18, 19]; it seems that there is still a great potential for ultra-downsizing yet [20].

A 50% downsized 3-cylinder engine optimal designing has been reported by Hancock et al. [21], focusing on design structure and employed technologies, and 30% fuel economy plus CO₂ reduction are reported as the

results of their optimal design. The concept of using pneumatic hybridization instead of electric ones for ultra-downsizing was reported more cost-efficient by Dönitz et al. [22]. The opportunity of a spark ignition engine 40% downsizing employing high octane bio-fuels and cooled Exhaust Gas Recirculated (EGR) was investigated by Splitter and Szybist [23]. Furthermore, charge cooling with a tracer-based two-line Planar Laser Induced Fluorescence (PLIF) technique in an optical Gasoline Direct Injection (GDI) engine was introduced as an idea to increase volumetric efficiency and Compression Ratio (CR) for downsized engine by Anbari et al. [24]. In addition, Turner et al. [25] have achieved 35% CO₂ reduction by designing a 60% downsized engine from a 5L, 8-cylinder V-type Jaguar Land Rover engine. More efficient turbulent flow at intake port in part load operation was achieved using a new design of intake system by Millo et al. [26]; while it was not realized at full load. Cooperating of this new design via advancing of Inlet Valve Closing (IVC) and employing turbocharger was introduced as an effective way to improve SI engines performance. In 2015, Severi et al. [27] asserted that 20% displacement volume reduction besides providing right-size engine maximum power of studied GDI engine is achievable via 11% piston bore reduction and using both engine boosting and spark advancing, in a numerical investigation. The concept of designing a boosted uni-flow scavenged direct injection gasoline engine to achieve more than 50% downsizing is demonstrated by Ma and Zhao [28] for a two stroke engine. Furthermore, friction loss investigation due to employing micro-geometry piston bearing [29] and oil pan design for modern downsized engine [30] were studied.

TABLE 1. The domain of recent-employed strategies on engine downsizing

	Strategy	Result	Reference
Engine Design	3 cylinder, Optimized design structure	30% fuel economy, CO ₂ reduction	Hancock et al. [21]
	Engine redesign	35% CO ₂ reduction, 60% downsizing	Turner et al. [25]
	Bore reduction	20% downsizing	Severi et al. [27]
Engine Components Design	Micro-geometry piston bearing	Frictional losses reduction, Torque enhancement	Wróblewski et al. [29]
	Oil pan design	Noise reduction	Liu et al. [30]
	Intake system	Part load operation improvement	Millo et al. [26]
Engine Management	EMS, Supercharger	35% CO ₂ reduction, 60% downsizing	Turner et al. [25]
	IVC advancing, Turbocharger	Part load operation improvement	Millo et al. [26]
	Bio-fuels, Cooled EGR	40% downsizing	Splitter and Szybist [23]
Other	Boosted uni-flow scavenged GDI	>50% downsizing	Ma and Zhao [28]
	Charge cooling with PLIF	Volumetric efficiency enhancement, CR increase	Anbari et al. [24]
	Pneumatic hybridization	Cost-efficient ultra-downsizing	Dönitz et al. [22]

This brief review showed that the employed methods on engine downsizing include a wide range of strategies. Recent-employed strategies are summarized in Table 1.

Investigation in the literature clearly showed the important role of engine downsizing on emission reduction. In the other hand, considering the trend line of the Iran-domestic industries besides the daily-increasing demand of releasing clean engines, may strongly portrait the need of downsized engines in Iran markets. In consequence, in this research, the Iranian national engine (EF7) was investigated for a feasibility study of downsizing. The Naturally Aspirated (NA) 4 cylinder engine was considered as the base engine, and a 25% downsized version was introduced using the cylinder reduction strategy (3 cylinder engine) besides utilizing turbocharger and VVT technologies. To achieve this aim, a one-dimensional model which is able to investigate the base engine performance as well as applying turbocharger, cylinder reduction, and VVT is employed. The model is equipped with a zero-dimensional combustion sub-model. Indeed, to evaluate the validity of numeric results, and experimental estimation of engine performance in 3-cylinder condition, the fuel cut-off strategy is applied to the one cylinder of 4 cylinder EF7 Turbo-Charged (TC) engine. Furthermore, the model results in fuel cut-offed mode were compared via experimental results for double validity check. The methodology of this research is shown in Figure 1.

2. MODEL DESCRIPTOPN

The investigation of mass and energy equations for each component, is mainly used in engine one dimensional (1D) simulation [31]. The engine performance is finally estimated by the combination of 1D simulation results and a zero-dimensional two-zone thermodynamic simulation of the combustion process. So, the model has illustrated in two subsections namely; component and combustion simulations. The schematic of operating model is shown in Figure 2.

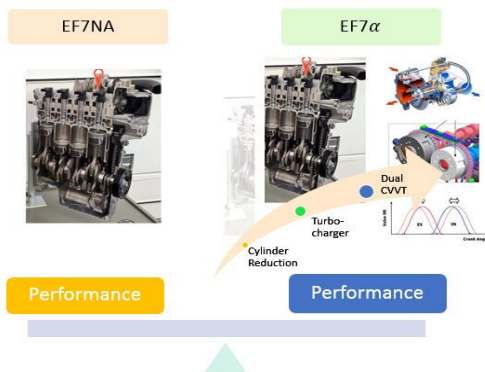


Figure 1. The methodology of this research

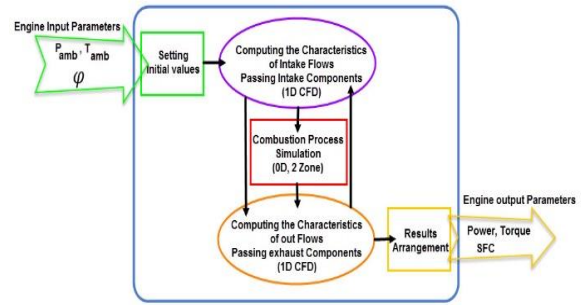


Figure 2. Schematic of one-dimensional component model with a zero-dimensional combustion sub-model

2. 1. Component Simulation

One-dimensional simulation needs to solve mass, energy and momentum equations, simultaneously. The trapped mass of each component is calculated by mass conservation equation [32]. The energy equation is expanded in transient form using work and convectional heat loss definitions [33] and momentum conservation equation is considered along with each component [32].

$$\dot{m}_{sub} = \sum \dot{m}_e - \sum \dot{m}_i \tag{1}$$

$$\frac{d(me)}{dt} = P \frac{dV}{dt} + \sum_i \dot{m}_i h_i - \sum_e \dot{m}_e h_e - h_g A (T_{gas} - T_{wall}) \tag{2}$$

$$\frac{\dot{m}}{dt} = \frac{dpA + \sum_i \dot{m}_i u + \sum_e \dot{m}_e u}{dx} - \frac{4 C_f \frac{\rho u^2}{2} \frac{dxA}{D} - C_p (\frac{1}{2} \rho u^2) A}{dx} \tag{3}$$

In these equations, \dot{m}_i and \dot{m}_e are the mass flow rates at the entrance and exit of each component which are defined as,

$$\dot{m} = \rho UA \tag{4}$$

where ρ , A , U indicate density, area and velocity of flow. Indeed, P , V , e , h , h_g , T_{gas} and T_{wall} in the energy equation are pressure, volume, specific internal energy, specific enthalpy, convection heat transfer coefficient, flow temperature and wall temperature, respectively. Convection heat transfer coefficient is described as:

$$h_g = \frac{1}{2} \rho C_f U_{eff} C_p Pr^{-\frac{2}{3}} \tag{5}$$

Here, C_f , U_{eff} , C_p and Pr define friction coefficient, effective velocity, specific heat coefficient and Prandtl number, respectively. Considering pipes roughness, the friction coefficient is defined by Nikuradse equation [34],

$$C_f(rough) = \frac{0.25}{(2 \log_{10}(\frac{1D}{2h}) + 1.74)^{0.25}} \tag{6}$$

where, D is the diameter of pipe and h is the height of roughness. In the momentum equation, C_p is pressure loss coefficient which is defined as:

$$C_p = \frac{P_i - P_e}{\frac{1}{2} \rho U_i^2} \tag{7}$$

Indexes i and e show inlet and outlet conditions.

2.2. Combustion Simulation A zero-dimensional two-zone thermodynamic model is employed for combustion process simulation. The combustion chamber is divided into the burned and unburned zones and the first law of thermodynamics, ideal gas equation of state besides engine geometrical correlations are applied on each zone. The schematic of the two-zone model is shown in Figure 3. It should be noted that the heat transferred between two zones is ignored and it is assumed that a proportion of charge, due to the Wiebe function, enters the burned zone in each time-step.

Heat release rate is also defined by the Wiebe function which is modified for gasoline blend combustion [35]

$$x_b = 1 - \exp\left(-Ea\left(\frac{\theta - \theta_{ig}}{\Delta\theta}\right)^{m+1}\right) \quad (8)$$

where, x_b , Ea , and θ_{ig} are the mass fraction of burnt fuel, activation energy, and spark time, respectively. Energy equation, assuming charge and combustion products as the ideal gases and considering SI combustion process, can be written as [35]:

$$\frac{d(M_B E_B)}{d\theta} + P \frac{dV_B}{d\theta} + Q_B = \eta \text{LHV} M_f \frac{dx_b}{d\theta} + h_U \frac{dM_U}{d\theta} \quad (9)$$

$$\frac{d(M_U E_U)}{d\theta} + P \frac{dV_U}{d\theta} + Q_U = h_U \frac{dM_U}{d\theta} \quad (10)$$

where, M , E , V , P , η , LHV , and h are the symbols of mass, internal energy, volume, pressure, combustion efficiency, the low heating value of fuel, and specific enthalpy and the indexed U and B refer to the unburnt and burnt zones. The heat transferred from the unburnt zone is equal to $x_b Q$. It is considered as $(1 - x_b)Q$ for the burnt zone, where Q is the total heat transfer from the Woschni correlation [36].

$$\frac{dQ}{d\theta} = h_c A_c \frac{dT}{d\theta} \quad (11)$$

$$h_c = 130 P^{0.8} U^{0.8} B^{-0.2} T^{-0.55} \quad (12)$$

Here, A_c , T , and U are the effective area of heat transfer,

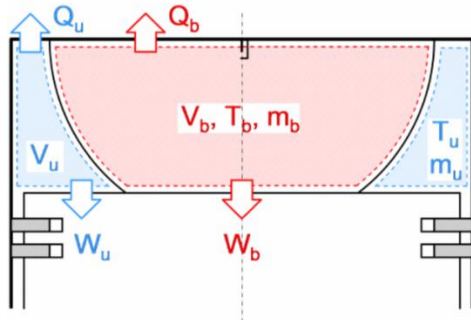


Figure 3. Schematic of two-zone combustion model

in-cylinder gas temperature, and gas local speed which is calculated by the mean piston velocity. It should be noted that the temperature of these equations are the mean cylinder temperature which is calculated as [35]:

$$T = \frac{x_b C_{v_B} T_B + (1 - x_b) C_{v_U} T_U}{x_b C_{v_B} + (1 - x_b) C_{v_U}} \quad (13)$$

C_v is the specific heat coefficient in constant volume and the volume of combustion chamber defined by engine geometrical correlation [35].

$$V = V_c + \frac{\pi B^2}{4} (l - a - a \cos(\theta) - \sqrt{l^2 - a^2 \sin^2(\theta)}) \quad (14)$$

Here, V_c , l , and a are the clearance volume, connecting rod length and crank radius, respectively and θ refers to the crank angle. The total volume is divided into the two burnt and unburnt sections, so the state equation of ideal gas for each zone is like;

$$\frac{PV_B}{RT_B} = M_B = x_b M_t \quad (15)$$

$$\frac{PV_U}{RT_U} = M_U = (1 - x_b) M_t \quad (16)$$

where, M_t refers to the total trapped mass in the cylinder. In addition to the noted correlations, there are some other considerations applied to the control volume due to the component type, its characteristics and operating conditions. Some of them are listed in the following;

- The velocity, turbulence, pressure loss and other features of charge flow would be affected by the valve lifting profile.
- The Continuous Variable Valve Timing (CVVT) is adopted from the engine operating map.
- The losses caused by the injection type would be affected by the characteristics of the injector such as static injection, dynamic injection, injection duration, injection timing, injection angle, and the number of nozzles. In this study, only the effect of the number of nozzles is ignored.
- The turbocharger is modelled by the own operating map which is provided by the producer, so the turbine rotational speed, efficiency, power and the boosted pressure are calculated by the amount of flow passing the turbine blades.
- The passing flow of turbine blades is controlled by the wastegate lifting profile which is adopted from the engine operating map.
- Ignition timing, fuel injected, and equivalence ratio are also adopted from the engine operating map.
- The friction loss of engine components is defined due to the engine frictional test.
- The compressor bypass flow, cyclic variations, angle of throttle, added fuel by canister valve, the losses by oil pump, water pump, alternator and other accessories are ignored due to the kind of simulation.

3. EXPERIMENTAL SETUP

The experimental tests were carried out in the Irankhodro Powertrain Company (IPCO). Two types of Iranian national engines, EF7, were available for the experimental test: Natural Aspirated (NA) and Turbocharged (TC). The main characteristics of the EF7 engines are reported in Table 2.

The schematic of the test room is shown in Figure 4 and also the accuracy of measurement instruments is reported in Table 3. Both of the engines are coupled with the AVL 220kW dynamometer which is controlled by the Puma controlling system and able to fix the engine speed by 1rpm accuracy. The utilized fuel flow meter, fuel temperature control system and blowby meter are licenced by the AVL company. Indeed, the combustion process is analyzed separately in the Indicom commercial software environment and the engine actuators are generally controlled by the other computer; thanks to employing open ECU and INCA commercial software. The used Horiba gas analyzer brings this opportunity that investigates the inlet air characteristics and measuring the equivalence ratio, in addition to evaluate the concentration of the exhaust gas species.

4. VALIDATION

To investigate the EF7 engine performance and also the capability of its downsizing, two one-dimensional

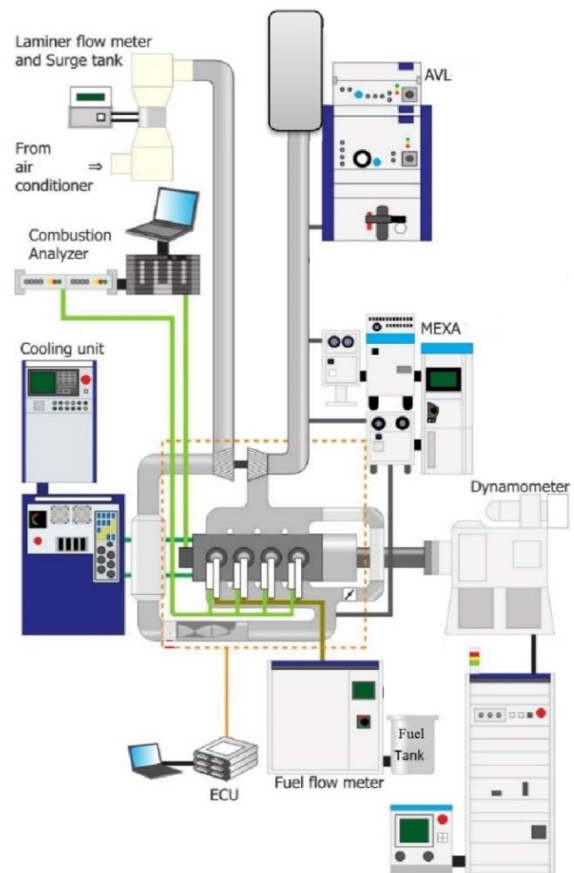


Figure 4. Test setup

TABLE 2. The main characteristics of EF7 engines

Engine name	EF7NA [37]	EF7TC [38]
Engine type	4 inline cylinder	
Bore × Stroke	78.6 × 85 mm	
Connection rod length	134.5 mm	
Compression Ratio	11	9.6
IVC	40 deg aBDC	26 deg aBDC
Exhaust Valve Opening (EVO)	50 deg bBDC	25 deg bBDC
Fuel	Gasoline	
CVVT	Intake	---

TABLE 3. Specifications of measurement instruments

Parameter	Accuracy
In-cylinder Pressure	±0.1 bar
Engine Speed	±1 rpm
Crank Angle	±0.1 CAD
Torque	±0.1 N.m
Fuel Consumption	0.12%
Equivalence Ratio	±0.02

models are provided using described equations at model description section within the GT-Power commercial software environment. The first model simulates the NA engine and the second one is developed to simulate TC engine performance.

The results of simulations for NA and TC engines at full load condition are compared with the experimental data. It should be noted that, all engine input parameters are adopted from the engine operating map. Brake torque, power, Mean Effective Pressure (BMEP), Specific Fuel Consumption (BSFC) in different engine speeds are considered as the main parameters for validation. The results for the NA engine showed the mean error of brake torque by 5.44%, specific fuel consumption by 2.74% and brake power by 4.22% illustrated in Figures 5 to 7. Simulated brake power, torque and also in-cylinder pressure variation are also compared via experimental results for TC engine shown in Figures 8 to 10; which show the mean error of 2.36% for brake power, 2.93% for brake torque and acceptable estimation of in-cylinder pressure. It should be noted that the experimental result for in-cylinder pressure is shown for the 500-cycles sample.

Considering Figures 5 to 10, it would be asserted that the provided models are reliable for both EF7NA and TC

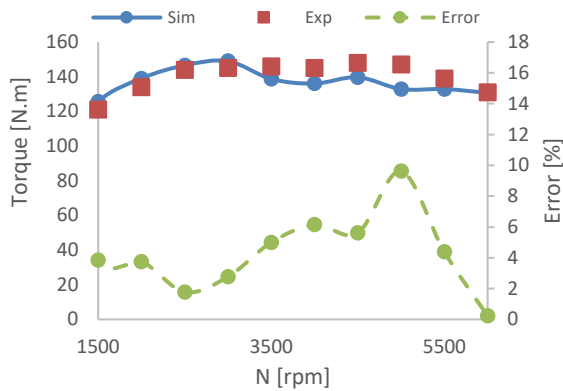


Figure 5. Simulated brake torque via experimental results for EF7NA

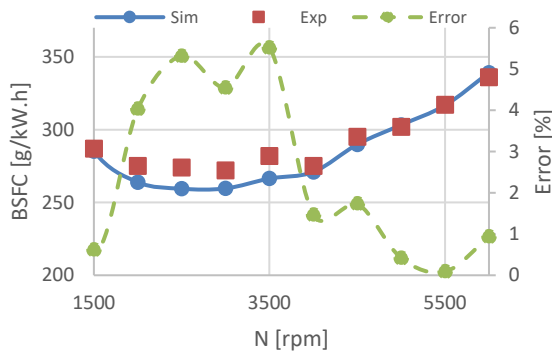


Figure 6. Simulated brake specific fuel consumption via experimental results for EF7NA

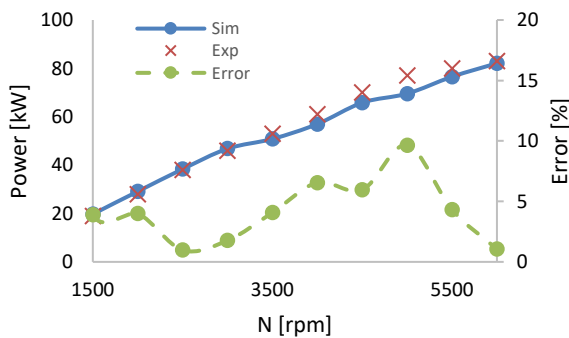


Figure 7. Simulated brake power via experimental results for EF7NA

engines performance evaluation, and also it can be used for feasibility study of downsizing.

5. RESULTS AND DISCUSSION

Gasoline fueled EF7NA engine is considered as the base engine for downsizing. The main objective of this study is to propose a downsized EF7 version employing the

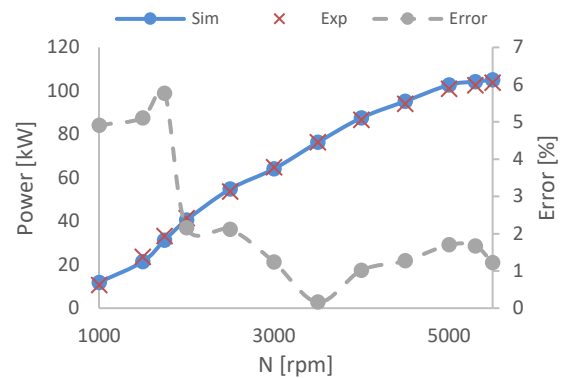


Figure 8. Simulated brake power via experimental results for EF7TC

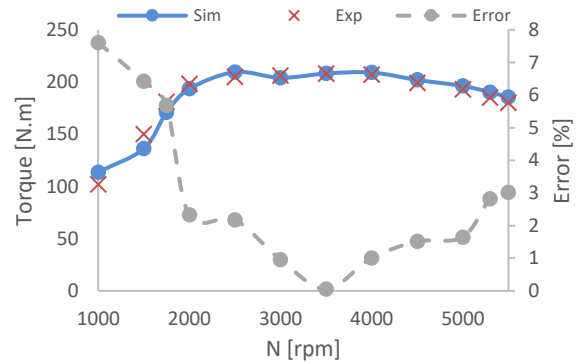


Figure 9. Simulated brake torque via experimental results for EF7TC

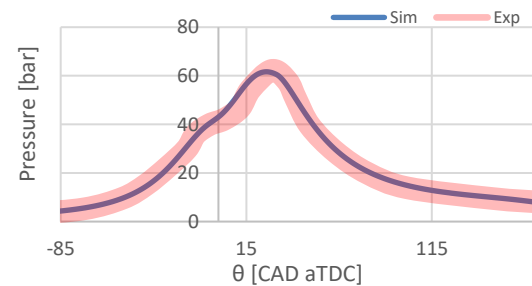


Figure 10. Simulated in-cylinder pressure via experimental results for EF7TC, N=5500 rpm

technology available in Iran. At first, considering the gasoline fueled EF7TC engine performance, a 3-cylinder gasoline fueled TC engine is introduced as the first conceptual version of downsized EF7 called EF7 α . In the next step, the role of employing different turbochargers is investigated to improve the performance of EF7 α . Finally, to achieve acceptable performance in low speed conditions, the effect of employing VVT is also studied. The main characteristics of the base engine besides EF7 α are reported in Table 4.

It should be noted that, in this step, the fuel cut-off strategy for a cylinder of EF7TC, is applied at the test setup to have an estimation of experimental performance of the 3-cylinder engine. In this study, the results of this strategy are called cylinder deactivated. However, the simulations are carried out for both strategies; cylinder deactivated and real 3-cylinder mode.

The concept of EF7 α is adopted by gasoline fueled EF7TC engine performance which is compared with NA one in Figure 11. As it is shown in Figure 11, the TC engine produces brake torque almost 1.33 times more than NA one. Consequently, it can be expected that EF7 α shows the same performance as the considered base engine. The results of simulations for both strategies; cylinder deactivated and real 3-cylinder mode are compared with the base engine shown in Figure 12. The results showed the well agreement with the noted assertion in case of cylinder deactivated and poor performance for 3-cylinder mode before 2800 rpm. The main reason of such a behavior is due to the noticeable reduction in the flow-rate passing turbine blades in case of 3-cylinder mode. However setting the right situation of the wastegate (considering the limitations such as knock, maximum boost pressure, maximum turbine inlet temperature and maximum turbine speed), the EF7 α provides the same torque as the base engine after 2800 rpm. The same challenges had been reported in the literature and different strategies were employed to tackle them [24, 26, 28].

TABLE 4. The basic data of base and downsized engines

Engine name	Base Engine	EF7 α
Engine type	4 inline cylinder	3 inline cylinder
	NA	TC
Bore \times Stroke	78.6 \times 85 mm	
Connection rod length	134.5 mm	
Compression ratio	11	9.6
Fuel	gasoline	
CVVT	Intake	Intake, Exhaust

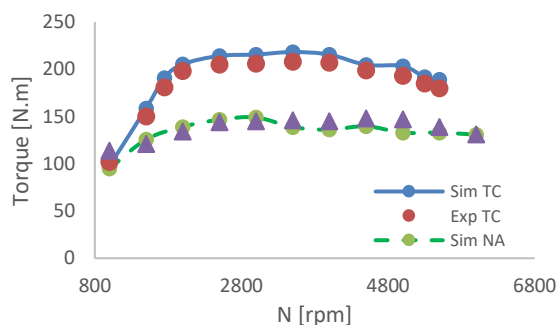


Figure 11. Brake torque comparison, EF7TC via EF7NA

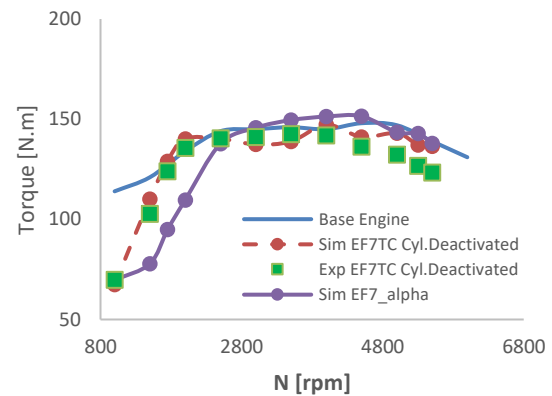


Figure 12. Brake torque comparison, EF7 α via base engine

Due to the Figure 12, it is obvious that to achieve better performance at low speed conditions, employing the turbocharger well-matched with EF7 α , is needed. To achieve this aim, a turbo-matching study is carried out based on the common turbochargers of Iran markets which are able to be installed on EF7. The basic information of investigated turbochargers is reported in Table 5. The operating maps of these turbochargers are applied to the model and the results are compared in Figure 13. Looking more detail in Figure 13, it can be asserted that from the investigated turbochargers, the F-Diesel one has the best performance matching with EF7 α which shifts the engine acceptable performance from >2800 rpm to >1900 rpm.

Although using the F-Diesel turbocharger the performance of EF7 α seems a better situation, the performance enhancement between 1000 to 1900 rpm is still needed. To achieve this aim, employing VVT technology can be considered as a promising solution. Consequently, the VVT sweep is carried out before 2000 rpm thanks to the ability of provided numerical model. In this approach dual CVVT is applied to the model and finally the best valve timing for each speed selected based on the maximum torque and minimum BSFC. The swept CVVTs at 1500 rpm are reported in Table 6. The candidate positions have shaded table cells and the desired CVVT are underlined in the table. The engine

TABLE 5. The information of investigated turbochargers

Case	Company	Model	Base Installed Engine
TC#1	Fuyuan	JEF7-3B	EF7TC, Commercial (Gasoline Fueled)
TC#2	Honeywell	C44-T79	EF7TC, Mule (Bi-Fueled)
TC#3		C46-T79	EF7TC, Mule (CNG Dedicated)
TC#4	F-Diesel	FD159-A016	EF7TC+, Mule (Gasoline Fueled)

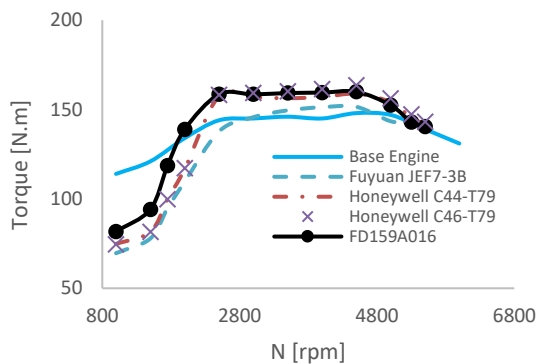


Figure 13. Brake torque comparison, EF7α with different turbochargers via base engine

behaviour shown in Table 6 is affected by different controlling/limiting parameters such as volumetric efficiency, real compression ratio, knock, spark timing, turbine inlet maximum temperature, turbine maximum rotational speed, maximum pressure/temperature in inlet port and allowed range of equivalence ratio. Although, each of these parameters may be the limiting issue to achieve more torque in a certain case, but in general, the main cause of such a behaviour is the variations of volumetric efficiency and real compression ratio due to

the valve overlap increase. As an example the trend of volumetric efficiency variation due to the change in CVVT shown in Figure 14, is the same of reported torque in Table 6. However, gained torque is affected by the other noted parameters simultaneously. The results of employing desired CVVT at the two speed conditions are shown in Figure 15, and it is clear that the provided torque of EF7α using optimum VVT and well-matched turbocharger is at least the same as the base engine. However, the provided torque at 1000 rpm is still estimated 7.01% lower than the base engine which is acceptable for a downsized engine [21].

The comparison of brake power is also shown the same trend for EF7α, and the engine is able to provide at least the same power as the base engine after 1500 rpm. However, the provided power at 1000 rpm is still estimated 4.5 kW lower than the base engine, as shown in Figure 16.

BMEP and BSFC of EF7α are also compared with the base engine, shown in Figures 17 and 18. It is obvious in both figures that the performance of EF7α in real 3-cylinder mode covers the base engine while there are significant differences for cylinder deactivated approach (32.5% decrease in BMEP and 57% increase in BSFC). These are related to the definition of these parameters that

TABLE 6. The swept CVVTs, and definition of desired VVT at 1500 rpm

	Exhaust=0		Exhaust=-17		Exhaust=-33		Exhaust=-52	
	Torque [N.m]	BSFC [g/kW.h]						
Intake =0	100.8	246.5	100.9	227.4	92.2	228.4	80.0	236.3
Intake =15	115.5	267.8	117.7	259.4	105.7	258.2	119.9	271.6
Intake =30	109.0	247.7	116.7	259.8	136.8	277.7	142.2	354.7
Intake =45	107.4	260.7	127.7	276.4	144.3	335.4	88.5	376.0
Intake =60	98.3	238.1	124.4	279.3	98.1	355.7	75.1	302.0

*CVVT Intake=0, Exhaust=0 is referred to the lock position which means no overlap for valve timing

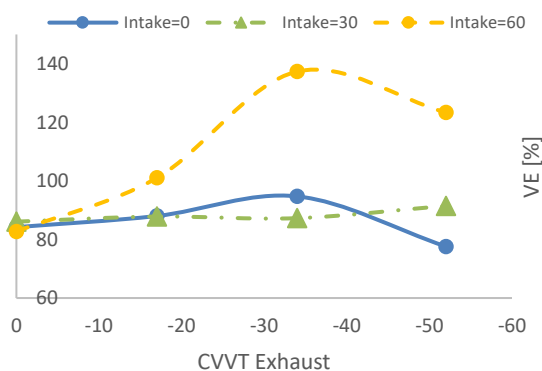


Figure 14. Volumetric efficiency variation via CVVT

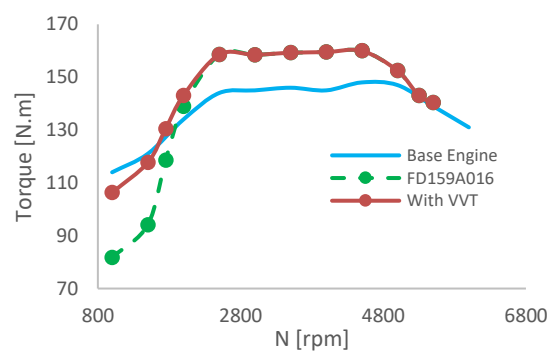


Figure 15. Brake torque comparison, EF7α with turbocharger and CVVT via base engine

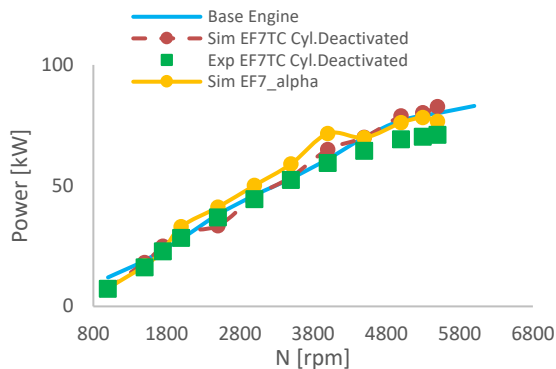


Figure 16. Brake power comparison, EF7 α via base engine

the reduction in fuel consumption is occurred just for a cylinder while the power loss increased by the frictional and pumping losses of the deactivated cylinder. Further than the lack of pumping loss of the deactivated cylinder, the frictional and inertial resistances due to the engine components such as camshaft are also removed in real 3-cylinder mode. Similarly, the effect of distance-volume reduction is not applied in cylinder deactivated approach.

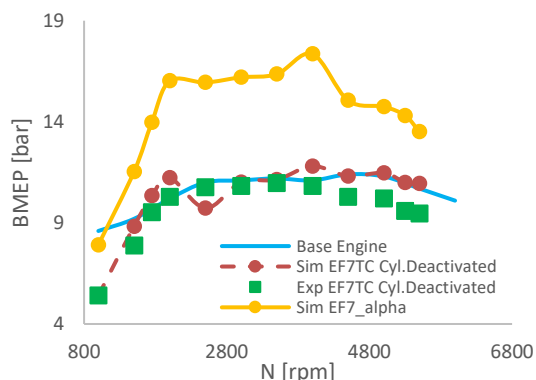


Figure 17. BMEP comparison, EF7 α via base engine

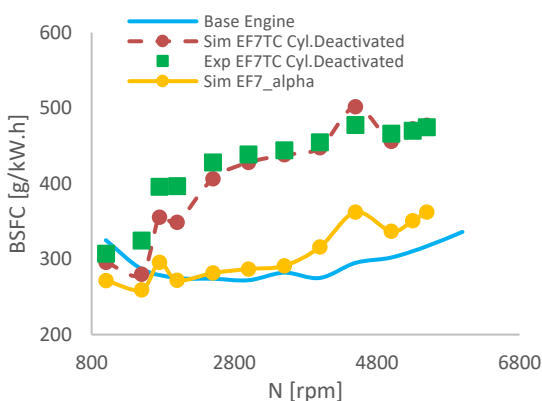


Figure 18. BSFC comparison, EF7 α via base engine

6. CONCLUSION

In this research the Iranian engine EF7NA is evaluated for 25% downsizing. Cylinder reduction besides using boost technologies namely; turbocharger and CVVT is the main employed strategy for this research. To investigate the downsized engine performance, two one-dimensional models equipped with a two-zone combustion sub-model and an experimental test cell are employed which are able to apply different strategies of this work. The main results are listed as follow:

- Provided models have enough accuracy to investigate the full load operation of both; NA and TC engines.
- Provided models are able to estimate the effect of using CVVT and different turbochargers.
- Both strategies; cylinder deactivation and cylinder reduction are applicable in the provided models.
- The 3-cylinder strategy employing F-Diesel as the well-matched turbocharger and CVVT can cover all the requirements as the downsized engine.
- EF7 α can be introduced as the first generation of Iranian downsized engine.

7. ACKNOWLEDGMENT

The authors wish to express their appreciation to the Irankhodro Powertrain Company (IPCO) for sharing necessary data during the course of this research.

8. REFERENCES

1. International Energy Agency. Policy pathways: improving the fuel economy of road vehicles – A policy package; 2011. <https://www.iea.org/publications/freepublications/publication/policy-pathways-improving-the-fuel-economy-of-road-vehicles---a-policy-package.html>
2. Zhang, W., Yang, X., Wang, T., Peng, X. and Wang, X., "Experimental study of a gas engine-driven heat pump system for space heating and cooling", *Civil Engineering Journal*, Vol. 5, No. 10, (2019), 2282-2295. <https://doi.org/10.28991/cej-2019-03091411>
3. Borowski, P.F., "New technologies and innovative solutions in the development strategies of energy enterprises", *High Tech and Innovation Journal*, Vol. 1, No. 2, (2020), 39-58. <https://doi.org/10.28991/HIJ-2020-01-02-01>
4. Topçuoğlu, K., "Trombe wall application with heat storage tank", *Civil Engineering Journal*, Vol. 5, No. 7, (2019), 1477-1489. <https://doi.org/10.28991/cej-2019-03091346>
5. Ravi, P., Devanandh, V., Pandey, S.K., Senthilnathan, K., Sadagopan, K. and Patel, B.P., Quasi-dimensional thermodynamic simulation study of downsizing on a four-cylinder turbocharged engine, *in Advances in Energy Research*, vol. 2, (2020), 563-575. https://doi.org/10.1007/978-981-15-2662-6_51
6. Namar, M.M., Jahanian, O., Shafaghat, R. and Nikzadfar, K., "Feasibility study for downsizing ef7 engine, numerical and experimental approach", *The Journal of Engine Research*, Vol.

- 61, No. 61, (2021), 73-85. <http://engineresearch.ir/article-1-758-en.html>
7. Cho, J., Kim, K., Baek, S., Myung, C.-L. and Park, S., "Abatement potential analysis on CO₂ and size-resolved particle emissions from a downsized lpg direct injection engine for passenger car", *Atmospheric Pollution Research*, Vol. 10, No. 6, (2019), 1711-1722. <https://doi.org/10.1016/j.apr.2019.07.002>
 8. Knauder, C., Allmaier, H., Sander, D.E. and Sams, T., "Investigations of the friction losses of different engine concepts. Part 2: Sub-assembly resolved friction loss comparison of three engines", *Lubricants*, Vol. 7, No. 12, (2019), 105. <https://doi.org/10.3390/lubricants7120105>
 9. Namar, M.M. and Jahanian, O., "Energy and exergy analysis of a hydrogen-fueled hcci engine", *Journal of Thermal Analysis and Calorimetry*, Vol. 137, No. 1, (2019), 205-215. <https://doi.org/10.1007/s10973-018-7910-7>
 10. Jafari, B., Khatamnejad, H., Shahavi, M.H. and Domeyri Ganji, D., "Simulation of dual fuel combustion of direct injection engine with variable natural gas premixed ratio", *International Journal of Engineering, Transactions C: Aspects*, Vol. 32, No. 9, (2019), 1327-1336. <https://dx.doi.org/10.5829/ije.2019.32.09c.14>
 11. Namar, M.M. and Jahanian, O., "A simple algebraic model for predicting hcci auto-ignition timing according to control oriented models requirements", *Energy Conversion and Management*, Vol. 154, (2017), 38-45. <https://doi.org/10.1016/j.enconman.2017.10.056>
 12. Hassanzadeh Saraei, S., Jafarmadar, S., Khalilarya, S. and Taghavifar, H., "Effects of triple injection strategies on performance and pollutant emissions of a di diesel engine using cfd simulation", *International Journal of Engineering, Transactions C: Aspects*, Vol. 31, No. 6, (2018), 973-979. <https://dx.doi.org/10.5829/ije.2018.31.06c.15>
 13. Kazemian, M. and Gandjalikhan Nassab, S., "Thermodynamic analysis and statistical investigation of effective parameters for gas turbine cycle using the response surface methodology", *International Journal of Engineering, Transactions B: Applications*, Vol. 33, No. 5, (2020), 894-905. <https://dx.doi.org/10.5829/ije.2020.33.05b.22>
 14. Hu, K. and Chen, Y., "Technological growth of fuel efficiency in european automobile market 1975–2015", *Energy Policy*, Vol. 98, (2016), 142-148. <https://doi.org/10.1016/j.enpol.2016.08.024>
 15. Merker, G.P., Schwarz, C. and Teichmann, R., "Combustion engines development: Mixture formation, combustion, emissions and simulation", *Springer Science & Business Media*, (2011). <https://doi.org/10.1007/978-3-642-14094-5>
 16. Kuhlbach, K., Mehring, J., Borrmann, D. and Friedfeld, R., "Zylinderkopf mit integriertem abgaskrümmer für downsizing-konzepte", *MTZ-Motortechnische Zeitschrift*, Vol. 70, No. 4, (2009), 286-293. <http://dx.doi.org/10.1007/BF03225480>
 17. Smith, A., "Stroke of genius for gasoline downsizing", *Ricardo Q Review*, (2008), https://scholar.google.com/scholar_lookup?title=Stroke+of+genius+for+gasoline+downsizing&publication_year=2008
 18. Budack, R., Wurms, R., Mendl, G. and Heiduk, T., "Der neue 2, 0-l-r4-tfsi-motor von audi", *MTZ-Motortechnische Zeitschrift*, Vol. 77, No. 5, (2016), 16-25. <http://dx.doi.org/10.1007/s35146-016-0035-2>
 19. Wang, Y., Wei, H., Zhou, L., Li, Y. and Liang, J., "Effect of injection strategy on the combustion and knock in a downsized gasoline engine with large eddy simulation", (2020), *SAE Technical Paper*. <https://doi.org/10.4271/2020-01-0244>
 20. Morikawa, K., Shen, F., Yamada, T., Moriyoshi, Y. and Kuboyama, T., "The extension of load range and low fuel consumption range based on the ultra-highly boosted downsized engine concept", *Transactions of Society of Automotive Engineers of Japan*, Vol. 51, No. 5, (2020). <https://doi.org/10.11351/jsaeronbun.51.862>
 21. Hancock, D., Fraser, N., Jeremy, M., Sykes, R. and Blaxill, H., "A new 3 cylinder 1.2 l advanced downsizing technology demonstrator engine" (2008), *SAE Technical Paper*. <https://doi.org/10.4271/2008-01-0611>
 22. Dönitz, C., Vasile, I., Onder, C. and Guzzella, L., "Realizing a concept for high efficiency and excellent driveability: The downsized and supercharged hybrid pneumatic engine", (2009), *SAE Technical Paper*, <https://doi.org/10.4271/2009-01-1326>
 23. Splitter, D.A. and Szybist, J.P., "Experimental investigation of spark-ignited combustion with high-octane biofuels and egr. 1. Engine load range and downsize downsized opportunity", *Energy & Fuels*, Vol. 28, No. 2, (2014), 1418-1431. <https://doi.org/10.1021/ef401574p>
 24. Attar, M.A., Herfatmanesh, M.R., Zhao, H. and Cairns, A., "Experimental investigation of direct injection charge cooling in optical gdi engine using tracer-based plif technique", *Experimental Thermal and Fluid Science*, Vol. 59, (2014), 96-108. <http://dx.doi.org/10.1016/j.expthermflusci.2014.07.020>
 25. Turner, J., Popplewell, A., Patel, R., Johnson, T., Darnton, N., Richardson, S., Bredda, S., Tudor, R., Bithell, C. and Jackson, R., "Ultra boost for economy: Extending the limits of extreme engine downsizing", *SAE International Journal of Engines*, Vol. 7, No. 1, (2014), 387-417. <https://doi.org/10.4271/2014-01-1185>
 26. Millo, F., Luisi, S., Borean, F. and Stroppiana, A., "Numerical and experimental investigation on combustion characteristics of a spark ignition engine with an early intake valve closing load control", *Fuel*, Vol. 121, (2014), 298-310. <https://doi.org/10.1016/j.fuel.2013.12.047>
 27. Severi, E., d'Adamo, A., Berni, F., Breda, S., Lugli, M. and Mattarelli, E., "Numerical investigation on the effects of bore reduction in a high performance turbocharged gdi engine. 3d investigation of knock tendency", *Energy Procedia*, Vol. 81, No., (2015), 846-855. <https://doi.org/10.1016/j.egypro.2015.12.094>
 28. Ma, J. and Zhao, H., "The modeling and design of a boosted uniflow scavenged direct injection gasoline (busdig) engine" (2015), *SAE Technical Paper*. <https://doi.org/10.4271/2015-01-1970>
 29. Wróblewski, E., Finke, S. and Babiak, M., "Investigation of friction loss in internal combustion engine of experimental microgeometry piston bearing surface", *Journal of KONES*, Vol. 24, (2017). <https://doi.org/10.5604/01.3001.0010.2951>
 30. Liu, J., Liu, Y. and Bolton, J.S., "The application of acoustic radiation modes to engine oil pan design" *SAE Technical Paper*, (2017), <https://doi.org/10.4271/2017-01-1844>
 31. Gamma Inc. Users Manual, volume 61. Gamma Technologies, 2004. <https://www.gtisoft.com/>
 32. White, F.M., Fluid mechanics, WCB. Ed McGraw-Hill Boston; 1999. https://books.google.com/books?id=fa_pAAAAMAAJ
 33. Sonntag RE, Borgnakke C, Van Wylen GJ, Van Wyk S. Fundamentals of thermodynamics. New York: Wiley; 1998. <https://books.google.com/books?id=95hVAAAAMAAJ>
 34. Nikuradse J. "Laws of flow in rough pipes", Washington: National Advisory Committee for Aeronautics; 1950 Nov 1. <https://citeseerx.ist.psu.edu/viewdoc/download?doi=10.1.1.467.2980&rep=rep1&type=pdf>
 35. Heywood JB. Internal Combustion Engine Fundamentals. 1st Edition, McGraw-Hill, 1988. <https://books.google.com/books?id=O69nQgAACAAJ>
 36. Woschni, G., "A universally applicable equation for the instantaneous heat transfer coefficient in the internal combustion engine" (1967), *SAE Technical Paper*, <https://doi.org/10.4271/670931>

37. Asgari, O., Hannani, S.K. and Ebrahimi, R., "Improvement and experimental validation of a multi-zone model for combustion and no emissions in cng fueled spark ignition engine", *Journal of Mechanical Science and Technology*, Vol. 26, No. 4, (2012), 1205-1212. <https://doi.org/10.1007/s12206-012-0229-6>
38. Gharloghy J, Kakaee A, Forooghifar A. Comparison of EF7 TC engine performance in two modes of CNG and petrol using piston and combustion chamber thermal simulation. *Fuel and Combustion*, (2011), Vol. 3, No. 2, 1-16. <https://www.sid.ir/en/journal/ViewPaper.aspx?ID=197151>

Persian Abstract

چکیده

کوچک سازی ابعادی به عنوان یک روش پذیرفته شده برای کاهش سوخت مصرفی و آلاینده‌گی موتورهای احتراق داخلی مطرح می‌باشد. در این پژوهش موتور ملی تنفس طبیعی EF7 به عنوان هدف کوچک سازی ابعادی انتخاب شده و در راستای ارائه یک نسخه ابعاد کوچک از آن تلاش شده است. بدین منظور از یک مدل عددی یک بعدی موتور استفاده شده که قابلیت اعمال استراتژی‌های مختلف شامل افزودن توربوشارژر، غیرفعال سازی یک سیلندر، حذف یک سیلندر و همچنین زمانبندی متغیر سوپاپ‌ها را دارد. به علاوه، به منظور صحت سنجی نتایج مدل، از یک بستر آزمایشگاهی جهت بررسی عملکرد موتور در حالت‌های تنفس طبیعی، توربوشارژ و یک سیلندر غیر فعال شده استفاده شده است. به منظور جبران ضعف عملکردی موتور ابعاد کوچک در دوره‌های پایین، تحلیل عملکرد موتور در ازای بکارگیری توربوشارژرهای مختلف و همچنین زمانبندی مختلف سوپاپ‌ها صورت پذیرفته و نتایج بدست آمده حاکی از آن است که موتور ابعاد کوچک معرفی شده، با بکارگیری توربوشارژر و زمانبندی بهینه سوپاپ‌ها می‌تواند گشتاوری معادل موتور پایه را ارائه دهد. حداکثر اختلاف گشتاور ارائه شده برابر با ۷ درصد و در دور ۱۰۰۰ دور بر دقیقه می‌باشد.
